View metadata, citation and similar papers at core.ac.uk
brought to you by CORE
provided by NASA Technical Reports Server

Input Constrained M-MRAC for Multirotors Operating in an Urban Environment

Vahram Stepanyan [1]
Universities Space Research Association, Columbia, MD 21046

Kalmanje Krishnakumar [2]
NASA Ames Research Center, Moffett Field, CA 94035

The paper presents a modified model reference adaptive control (M-MRAC) for multi-input multi-output nonlinear dynamical systems with time varying parametric uncertainties and bounded external disturbances. It uses a prediction model to rapidly generate adaptive estimates of the system's uncertainties with adjustable errors that converge to a small neighborhood of the origin. A sufficient condition is derived to specify the region of attraction in the space of initialization errors, design parameters and external commends. The approach is applied to thrust controlled multi-rotor air vehicles operating in an urban environment. It is shown that the designed controller can provide a good tracking of a given trajectory in the unknown urban wind field, assuming that the maximum thrust generated by the rotors is known. The performance of the algorithms are demonstrated in simulations.

I. Introduction

Multi-rotor air vehicles are becoming increasingly popular for civilian operations such as package delivery, inspection, security and disaster management due to their affordability and capability to

[1] Principal Scientist, NASA Ames Research Center/Mail Stop 269/1, AIAA Senior Member, email: vahram.stepanyan@nasa.gov
[2] Technical Lead, Intelligent Systems Division, NASA Ames Research Center/Mail Stop 269/3, AIAA Associate Fellow, email: kalmanje.krishnakumar@nasa.gov

operate in confined volumes (see for example [1, 7, 9, 14] and references therein). These vehicles have a small size, light weight structure and limited power, which makes them vulnerable to disturbances, especially when flying in a complex urban wind field, which is hard to predict and needs to be handled in flight. In addition, some operational conditions may demand control signals beyond the vehicle's physical limitations, which will result in performance degradations or even drive the vehicle into instability. Therefore, input constraint adaptive control design is critical for safety and reliability of these small UAV operations.

The adaptive control design for uncertain systems with input constraints has been a research topic for vast amount of publications both from design and analysis perspective. Some earlier results can be found in a review paper [3]. The main interest in control design of this type of systems is to prevent the adaptation mechanism to lead the system to instability when the control input hits the saturation limits. One way of addressing this issue is to modify the external command or the reference model dynamics such that the generated control signal remains in the given limits. Pseudo control hedging [6] and positive μ-modification [11] are based on this approach.

Other approaches use neural networks based control [4, 8, 10, 15], adaptive model predictive control [2], reference governors [12], adaptive anti-windup technique [5], adaptive backstepping control [19, 21, 22], convex optimization of the quadratic retrospective cost function [20], just to mention few of them. In these approaches designed controllers achieve bounded tracking in the presence of parametric uncertainties and external disturbances under specific assumptions. In [8], it is assumed that the open-loop plant is locally stable, and bounded tracking of closed-loop system is ensured in local sense. In [2], it is assumed that nonlinearities are locally Lipschitz and the uncertain parameters are in known compact set. In [12], a reference governor is designed to modify the evolution of control signal to satisfy specified constraints. In [5], an adaptive anti-windup design is presented for single input systems in strict feedback form, and a piecewise linear approximation network is used to estimate the uncertainties with known bounds. In [19], a smooth approximation of the saturation function and Nussbaum gain based adaptive backstepping design is presented to achieve bounded tracking of a smooth command for input-to-state stable nonlinear uncertain systems in feedback form. In [20], the control signal limits are ensured by bounding the magnitude

of retrospectively optimized input signal for discrete-time linear systems under a set of assumptions. In [13], adaptive neural network backstepping control is designed for uncertain nonlinear systems in strict-feedback form with asymmetric saturation and external disturbances by using Gaussian error function-based continuously differentiable approximation of saturation and dynamic surface control to achieve a semi-global bounded tracking of a smooth command. In [4], a nonlinear disturbance observer and dynamic surface control based neural network backstepping is used for uncertain strict-feedback nonlinear systems to guarantee ultimately bounded convergence of all closed-loop signals. In [22] and [21], an auxiliary system combined with a command filter is designed to deal with the input saturation effect and achieve bounded tracking.

In this paper, we present an adaptive control method for input constraint multi-input multi-output nonlinear dynamical systems with time varying parametric uncertainties and bounded external disturbances. The method, which was first presented in [17], uses a prediction model to rapidly generate adaptive estimates of the system's uncertainties. It is shown that the designed controller requires no modification or tuning to guarantee tracking of a given reference model inside a region in the space of initialization errors, design parameters and external commends described by a sufficient condition, which is derived based on the adaptive estimation bounds. The approach is applied to control of thrust-limited multi-rotor air vehicles operating in an urban environment. It is shown that the designed controller can provide a good tracking of a given trajectory in the unknown urban wind field, assuming that the maximum thrust generated by the rotors is known. Verification of the presented algorithm is conducted using simulations.

II. Problem Statement

Let the desired behavior of a controlled system be represented by the reference model

$$\dot{\boldsymbol{x}}_m(t) = A\boldsymbol{x}_m(t) + B\boldsymbol{r}(t), \quad \boldsymbol{x}_m(0) = \boldsymbol{x}_{m0} \tag{1}$$

where $A \in R^{n\times n}$ is a Hurwitz matrix, $B \in R^{n\times q}$ and $\boldsymbol{r} : R^+ \to R^q$ is a bounded and piecewise continuous external command with a bounded derivative. Let the dynamics of the control system

be given by

$$\begin{aligned}\dot{\boldsymbol{x}}(t) &= A_0\boldsymbol{x}(t) + B_0\left[\boldsymbol{u}(t) + K_0\boldsymbol{g}(\boldsymbol{x}(t)) + \boldsymbol{d}(t)\right], \\ \dot{\boldsymbol{u}}(t) &= \boldsymbol{s}(\boldsymbol{u}(t), \boldsymbol{x}(t), \boldsymbol{v}(t))\end{aligned} \tag{2}$$

with $\boldsymbol{x}(0) = \boldsymbol{x}_0$, where $\boldsymbol{x} \in R^n$ is the state of the system, $\boldsymbol{g}(\boldsymbol{x}$ is known Lipschitz continuous nonlinear function, $\boldsymbol{u} \in R^q$ is the actuator's output, which is assumed to be available form direct measurements or form the model. For majority of control systems the actuator dynamics are fast enough to be replaced by a static map

$$\boldsymbol{u}(t) = \boldsymbol{h}(\boldsymbol{x}(t), \boldsymbol{v}(t)),$$

where $\boldsymbol{v}$ is the actuator's input. In essence, this map resembles the input constraint for the controlled system, which in many cases is just a saturation function (see for example [11] and references therein). The system's uncertainties are represented by matrices $A_0 \in R^{n\times n}$ and $B_0 \in R^{n\times q}$, $K_0 \in R^{q\times p}$ and the external disturbance $\boldsymbol{d} : R^+ \to R^q$, which satisfies the conditions

$$\|\boldsymbol{d}(t)\|_{\mathcal{L}_\infty} \le d^*,\ \|\dot{\boldsymbol{d}}(t)\|_{\mathcal{L}_\infty} \le d_d^*.$$

We assume that the matching conditions are satisfied, that is $A_0 = A + B_0K$ for some unknown K and $B_0 = B\Lambda$ for some unknown positive definite Λ, therefore the system (2) can be represented in the following form

$$\dot{\boldsymbol{x}}(t) = A\boldsymbol{x}(t) + B\boldsymbol{r}(t) + B\Lambda\left[\boldsymbol{u}(t) + \Theta\boldsymbol{f}(\boldsymbol{x}, \boldsymbol{r}) + \boldsymbol{d}(t)\right], \tag{3}$$

where we denote $\Theta\boldsymbol{f}(\boldsymbol{x}, \boldsymbol{r}) = K\boldsymbol{x} + K_0\boldsymbol{g}(\boldsymbol{x}) - \Lambda^{-1}\boldsymbol{r}$. Our approach permits to extend the problem formulation to time varying uncertainties $\Lambda(t)$ and $\Theta(t)$, which satisfy the conditions

$$\begin{aligned}&\|\Lambda(t)\|_{\mathcal{L}_\infty} \le \lambda^*,\ \|\Theta(t)\|_{\mathcal{L}_\infty} \le \vartheta^* \\ &\|\dot{\Lambda}(t)\|_{\mathcal{L}_\infty} \le \lambda_d^*,\ \|\dot{\Theta}(t)\|_{\mathcal{L}_\infty} \le \vartheta_d^*.\end{aligned} \tag{4}$$

The objective is to design actuator's input signal $\boldsymbol{v}(t)$ such that the system tracks the reference model (1) in the presence of time varying uncertainties and input constraints, which is assumed to

be a saturation function

$$u_i(t) = h_i(v_i(t)) = sat(v_i(t)) = \begin{cases} v_i^* \text{sign}(v_i), & if\ |v_i(t)| > v_i^* \\ \\ v_i(t), & if\ |v_i(t)| \leq v_i^* \end{cases},$$

in each channel, where $v_i^*,\ (i = 1, \ldots, q)$ is the maximum achievable value.

III. Prediction Model

To estimate the systems uncertainties we introduce the following prediction model

$$\dot{\hat{\boldsymbol{x}}}(t) = A\hat{\boldsymbol{x}}(t) + B\boldsymbol{r}(t) + B\hat{\Lambda}(t)[\boldsymbol{u}(t) + \hat{\Theta}(t)\boldsymbol{f}(\boldsymbol{x}, \boldsymbol{r}) + \hat{\boldsymbol{d}}(t)] + k\tilde{\boldsymbol{x}}(t) \tag{5}$$

with $\hat{\boldsymbol{x}}(0) = \hat{\boldsymbol{x}}_0$, where $\tilde{\boldsymbol{x}}(t) = \boldsymbol{x}(t) - \hat{\boldsymbol{x}}(t)$ is the prediction error, $k > 0$ is a design parameter, $\hat{\Lambda}(t)$, $\hat{\Theta}(t)$ and $\hat{\boldsymbol{d}}(t)$ are the estimates of the unknown quantities. We notice that the prediction model mimics the system's dynamics with uncertainties replaced with their estimates, assuming that the actuators output is available. When the map $\boldsymbol{u}(t) = \boldsymbol{h}(\boldsymbol{v}(t))$ is one-to-one, that is the function $\boldsymbol{h}(\boldsymbol{v}(t))$ can be inverted, then the actuator's output can be directly set to

$$\boldsymbol{u}_c(t) = -\hat{\Theta}(t)\boldsymbol{f}(\boldsymbol{x}, \boldsymbol{r}) - \hat{\boldsymbol{d}}(t) \tag{6}$$

by designing the control signal $\boldsymbol{v}(t)$ as

$$\boldsymbol{v}(t) = \boldsymbol{h}^{-1}\left(\boldsymbol{u}_c(t)\right) . \tag{7}$$

In this case, the prediction model reduces to the modified reference model

$$\dot{\hat{\boldsymbol{x}}}(t) = A\hat{\boldsymbol{x}}(t) + B\boldsymbol{r}(t) + k\tilde{\boldsymbol{x}}(t) . \tag{8}$$

This is the case of unconstrained M-MRAC with time variant uncertainties, which was studied in [17].

When the function $\boldsymbol{h}(\boldsymbol{v}(t))$ is not invertible, as in the case of saturation function, there is a discrepancy $\Delta\boldsymbol{u}(t) = \boldsymbol{u}(t) - \boldsymbol{v}(t)$ between the achieved control signal $\boldsymbol{u}(t)$ and demanded control signal $\boldsymbol{v}(t)$, and the prediction model is written as

$$\dot{\hat{\boldsymbol{x}}}(t) = A\hat{\boldsymbol{x}}(t) + B\boldsymbol{r}(t) + k\tilde{\boldsymbol{x}}(t) + B\hat{\Lambda}(t)\Delta\boldsymbol{u}(t) . \tag{9}$$

.

To complete the prediction model definition, we introduce the adaptive update laws for on-line parameter estimates as

$$\begin{aligned}
\dot{\hat{\Theta}}(t) &= \gamma \Pr\left(\hat{\Theta}(t),\ \tilde{\boldsymbol{y}}(t)\boldsymbol{f}^\top(\boldsymbol{x},\boldsymbol{r})\right) \\
\dot{\hat{\Lambda}}(t) &= \gamma \Pr\left(\hat{\Lambda}(t),\ \tilde{\boldsymbol{y}}(t)[\boldsymbol{u}(t)+\hat{\Theta}(t)\boldsymbol{f}(\boldsymbol{x},\boldsymbol{r})+\hat{\boldsymbol{d}}(t)]^\top\right) \\
\dot{\hat{\boldsymbol{d}}}(t) &= \gamma \Pr\left(\hat{\boldsymbol{d}}(t),\ \tilde{\boldsymbol{y}}(t)\right) ,
\end{aligned} \tag{10}$$

where $\gamma > 0$ is the adaptation rate, $\tilde{\boldsymbol{y}}(t) = B^\top P\tilde{\boldsymbol{x}}(t)$, $P = P^\top > 0$ is the solution of the Lyapunov equation $A^\top P + PA = -Q$ for some $Q = Q^\top > 0$, and $\Pr(\cdot,\cdot)$ denotes the projection operator [16].

IV. Prediction Error Bounds

In this section we obtain prediction error bounds, which are independent of the control design. To this end, we derive the error dynamics by substantiating (5) from (2)

$$\begin{aligned}
\dot{\tilde{\boldsymbol{x}}}(t) &= (A-k\mathbb{I})\tilde{\boldsymbol{x}}(t) + B\Lambda(t)[\tilde{\Theta}(t)\boldsymbol{f}(\boldsymbol{x},\boldsymbol{r}) + \tilde{\boldsymbol{d}}(t)] \\
&+ B\tilde{\Lambda}(t)[\boldsymbol{u}(t)+\hat{\Theta}(t)\boldsymbol{f}(\boldsymbol{x},\boldsymbol{r})+\hat{\boldsymbol{d}}(t)] ,
\end{aligned} \tag{11}$$

where $\tilde{\Theta}(t) = \Theta(t) - \hat{\Theta}(t)$, $\tilde{\Lambda}(t) = \Lambda(t) - \hat{\Lambda}(t)$ and $\tilde{\boldsymbol{d}}(t) = \boldsymbol{d}(t) - \hat{\boldsymbol{d}}(t)$ are the parameter estimation errors.

First of all, we notice that the projection operators in the adaptive laws (10) guarantee the following inequalities

$$\|\hat{\Theta}(t)\| \le \vartheta^*, \quad \|\hat{\Lambda}(t)\| \le \lambda^*, \quad \|\hat{\boldsymbol{d}}(t)\| \le d^* ,$$

which imply that

$$\|\tilde{\Theta}(t)\| \le 2\vartheta^*, \quad \|\tilde{\Lambda}(t)\| \le 2\lambda^*, \quad \|\tilde{\boldsymbol{d}}(t)\| \le 2d^* .$$

Therefore one can easily compute that

$$\tilde{\boldsymbol{d}}^\top(t)\Lambda(t)\tilde{\boldsymbol{d}}(t) + \mathrm{tr}\left(\tilde{\Theta}^\top(t)\Lambda(t)\tilde{\Theta}(t) + \tilde{\Lambda}^\top(t)\tilde{\Lambda}(t)\right) \le 4\lambda^* d^{*2} + 4\lambda^*\vartheta^{*2} + 4\lambda^{*2} \triangleq c_1 \tag{12}$$

and

$$\begin{aligned}
2\mathrm{tr}\left(\dot{\Theta}^\top(t)\Lambda(t)\tilde{\Theta}(t)\right) + 2\dot{\boldsymbol{d}}^\top(t)\Lambda(t)\tilde{\boldsymbol{d}}(t) + \tilde{\boldsymbol{d}}^\top(t)\dot{\Lambda}(t)\tilde{\boldsymbol{d}}(t) + \mathrm{tr}\left(\tilde{\Theta}^\top(t)\dot{\Lambda}(t)\tilde{\Theta}(t)\right) \\
\le 4\lambda^*\vartheta^*\vartheta_d^* + 4\lambda^* d^* d_d^* + 4\lambda_d^* d^{*2} + 4\lambda_d^*\vartheta^{*2} \triangleq c_2 .
\end{aligned} \tag{13}$$

Next, it is shown that the prediction error $\tilde{\boldsymbol{x}}(t)$ satisfies the bound

$$\|\tilde{\boldsymbol{x}}(t)\| \leq \sqrt{\frac{|V(0)-\frac{c}{\gamma}|}{\lambda_{\min}(P)}}e^{-kt} + \sqrt{\frac{c}{\gamma\lambda_{\min}(P)}}\,, \tag{14}$$

where $c = c_1 + \frac{c_2}{2k}$, and $V(0)$ is the initial value of the quadratic function

$$V(t) = \tilde{\boldsymbol{x}}^\top(t)P\tilde{\boldsymbol{x}}(t) + \gamma^{-1}\tilde{\boldsymbol{d}}^\top(t)\Lambda(t)\tilde{\boldsymbol{d}}(t) + \gamma^{-1}\mathrm{tr}\left(\tilde{\Theta}^\top(t)\Lambda(t)\tilde{\Theta}(t) + \tilde{\Lambda}^\top(t)\tilde{\Lambda}(t)\right)\,, \tag{15}$$

and $\lambda_{\min}(P)$ denotes the minimum eigenvalue of P. To this end, we compute the derivative of $V(t)$ along the trajectories of the prediction error dynamics (11) and the adaptive laws (10), and arrive the inequality

$$\dot{V}(t) \leq -\tilde{\boldsymbol{x}}^\top(t)Q\tilde{\boldsymbol{x}}(t) - 2k\tilde{\boldsymbol{x}}^\top(t)P\tilde{\boldsymbol{x}}(t) + \gamma^{-1}c_2\,. \tag{16}$$

On the other hand, $V(t) \leq \tilde{\boldsymbol{x}}^\top(t)P\tilde{\boldsymbol{x}}^\top(t) + \gamma^{-1}c_1$. Therefore,

$$\dot{V}(t) \leq -2k[V(t) - \gamma^{-1}c_1] + \gamma^{-1}c_2\,, \tag{17}$$

integration of which results in

$$V(t) \leq \left[V(0) - \frac{c}{\gamma}\right]e^{-2kt} + \frac{c}{\gamma}\,. \tag{18}$$

Noticing that $\|\tilde{\boldsymbol{x}}(t)\|^2 \leq V(t)/\lambda_{\min}(P)$, we readily obtain

$$\|\tilde{\boldsymbol{x}}(t)\| \leq \sqrt{\frac{1}{\lambda_{\min}(P)}}\sqrt{\left[V(0) - \frac{c}{\gamma}\right]e^{-2kt} + \frac{c}{\gamma}}\,, \tag{19}$$

which results in (14) taking into account the inequality $\sqrt{a+b} \leq \sqrt{a} + \sqrt{b}$ for any $a \geq 0,\ b \geq 0$.

It can be observed that the effect of prediction model initialization error decays exponentially with the rate k, which is assumed to be a large value for the fast adaptation. Therefore, we can set $\hat{\boldsymbol{x}}_0 = \boldsymbol{x}_0$, which reduces (14) to

$$\|\tilde{\boldsymbol{x}}(t)\| \leq \sqrt{\frac{c}{\gamma\lambda_{\min}(P)}}\,, \tag{20}$$

V. Performance bounds

First we derive the performance bounds assuming that the system is known. In this case, the control signal demand is given by the equation

$$\boldsymbol{v}_0(t) = -\Theta(t)\boldsymbol{f}(\boldsymbol{x},\boldsymbol{r}) - \boldsymbol{d}(t)\,, \tag{21}$$

which reduces the system into the reference model provided that $|v_i(t)| \leq v_i^*,\ (i = 1, \ldots, q)$ for all $t \geq 0$. That is the system's state and the external command satisfy the inequality

$$\| - K\boldsymbol{x} - K_0\boldsymbol{g}(\boldsymbol{x}) - \Lambda^{-1}\boldsymbol{r} - \boldsymbol{d}(t)|| \leq v^* \,, \tag{22}$$

where $v^* = \sqrt{q}\max_{i=1,\ldots,q}(v_i^*)$ (see [11] for details). In this case, the tracking error $\boldsymbol{e}(t) = \boldsymbol{x}(t) - \boldsymbol{x}_m(t)$ satisfies the exponentially stable dynamics

$$\dot{\boldsymbol{e}}(t) = A\boldsymbol{e}(t)\,, \tag{23}$$

the state transition matrix of which is bounded as $\|\exp(At)\| \leq \gamma_A \exp(-\lambda_A t)$. Therefore, $\|\boldsymbol{e}(t)\| \leq \gamma_A\|\boldsymbol{e}(0)\|$ for all $t \geq 0$. Similarly, the reference model satisfies the bound

$$\|\boldsymbol{x}_m(t)\| \leq \gamma_A \left(\|\boldsymbol{x}_m(0)\| + \lambda_A^{-1}||B\|r^*\right) \triangleq x_m^*,$$

where r^* is the external command bound. Substituting $\boldsymbol{x}(t) = \boldsymbol{e}(t) + \boldsymbol{x}_m(t)$ in (22) and taking into account Lipschitz condition $\|\boldsymbol{g}(\boldsymbol{x}) - \boldsymbol{g}(\boldsymbol{x}_m)\| \leq \lambda_g(\|\boldsymbol{e}\|)$, we obtain a sufficient condition for $\|\boldsymbol{v}_0(t)\| \leq v^*$ as

$$(\|K\| + \lambda_g\|K_0\|)\,\|\boldsymbol{x}_m(t)\| + \|K_0\|\|\boldsymbol{g}(x_m(t))\| + \gamma_A\,(\|K\| + \lambda_g\|K_0\|)\,\|\boldsymbol{e}(0)\| + \frac{\|\boldsymbol{r}(t)\|}{\lambda^*} + d^* \leq v^* \,. \tag{24}$$

The inequality (24) defines the region of attraction in terms of reference model state and initialization error, external command and disturbance bounds. It depends on design (reference model) parameters set by the user and on the bounds of unknown parameters $K,\ K_0, \Lambda,\ d$, which are also used to set the projection operator in the definition of adaptive laws (10). Therefore, given the system's initial condition $\boldsymbol{x}(0)$ and the reference model initialization error $\boldsymbol{e}(0)$, for any external command satisfying

$$(\|K\| + \lambda_g\|K_0\|)\,\|\boldsymbol{x}_m(t)\| + \|K_0\|\|\boldsymbol{g}(x_m(t))\| + \frac{\|\boldsymbol{r}(t)\|}{\lambda^*} \leq v^* - d^* - \gamma_A\,(\|K\| + \lambda_g\|K_0\|)\,\|\boldsymbol{e}(0)\| \,, \tag{25}$$

the system exponentially tracks the reference model with the control signal defined in (21), which will never violate the saturation limits provided that the right hand side of (25) is positive.

We notice that, when the adaptive control signal

$$\boldsymbol{v}(t) = -\hat{\Theta}(t)\boldsymbol{f}(\boldsymbol{x}, \boldsymbol{r}) - \hat{\boldsymbol{d}}(t)\,, \tag{26}$$

takes on values inside the actuator limits, then $\boldsymbol{u}(t) = \boldsymbol{v}(t)$ and prediction model (5) reduces to the modified reference model (see [17] for details)

$$\dot{\hat{\boldsymbol{x}}}(t) = A\hat{\boldsymbol{x}}(t) + B\boldsymbol{r}(t) + k\tilde{\boldsymbol{x}}(t)\,. \tag{27}$$

Hence the following bound can be easily derived

$$\|\hat{\boldsymbol{x}}(t) - \boldsymbol{x}_m(t)\| \leq \gamma_A \|\hat{\boldsymbol{x}}(0) - \boldsymbol{x}_m(0)\|| + \frac{\gamma_A k}{\lambda_A}\sqrt{\frac{c}{\gamma\lambda_{\min}(P)}}\,, \tag{28}$$

which implies that $\hat{\boldsymbol{x}}(t)$ is bounded, hence the uncertain system state $\boldsymbol{x}(t)$ remains bounded when the adaptive control is applied. In this case, the tracking error satisfies

$$\|\boldsymbol{e}(t)\| \leq \|\tilde{\boldsymbol{x}}(t)\| + \|\hat{\boldsymbol{x}}(t) - \boldsymbol{x}_m(t)\| \leq \gamma_A \|\hat{\boldsymbol{x}}(0) - \boldsymbol{x}_m(0)\|| + \left(\frac{\gamma_A k}{\lambda_A} + 1\right)\sqrt{\frac{c}{\gamma\lambda_{\min}(P)}}\,, \tag{29}$$

To derive sufficient conditions for the adaptive control to satisfy $\|\boldsymbol{v}(t)\| \leq v^*$ for all $t \geq 0$, we estimate the control difference $\tilde{\boldsymbol{v}}(t) = \boldsymbol{v}_0(t) - \boldsymbol{v}(t) = -\tilde{\Theta}(t)\boldsymbol{f}(\boldsymbol{x}, \boldsymbol{r}) - \boldsymbol{d}(t) + \hat{\boldsymbol{d}}(t)$. Following the steps from [17], it can be shown that $\tilde{\boldsymbol{v}}(t)$ satisfies the bound

$$\|\tilde{\boldsymbol{u}}(t)\| \leq \beta_1 e^{-\nu_1 t} + \beta_2 \gamma^{-\frac{1}{2}}\,, \tag{30}$$

where the positive constants ν_1, β_1 and β_2 are are defined in [17] and depend on design parameters, the unknown parameter bounds and the estimates initialization errors. Therefore, to ensure that the adaptive control $\boldsymbol{v}(t)$ does not violate the saturation limits, we require that it satisfies the conservative bound $\|\boldsymbol{v}(t)\| \leq v^* - \beta_1 - \beta_2 \triangleq \bar{v}$. That is, given the system's initial condition $\boldsymbol{x}(0)$ and the reference model initialization error $\boldsymbol{e}(0)$, for any external command satisfying

$$(\|K\| + \lambda_g\|K_0\|)\,\|\boldsymbol{x}_m(t)\| + \|K_0\|\|\boldsymbol{g}(x_m(t))\| + \frac{\|\boldsymbol{r}(t)\|}{\lambda^*} \leq \bar{v} - d^* - \gamma_A\,(\|K\| + \lambda_g\|K_0\|)\,\|\boldsymbol{e}(0)\|\,, \tag{31}$$

the system tracks the reference model with an error satisfying the bound (29), provided that the right hand side of (31) is positive. The following theorem summarizes the sufficient condition, under which the tracking error satisfies the bound (29).

Theorem V.1 *Consider the system (2), reference model (1), prediction model (5), adaptive control (26) and the adaptive laws (10). If the external disturbance satisfies the condition* $v^* - \beta_1 - \beta_2 - d^* - \rho_1 > 0$ *for some* $\rho_1 > 0$*, the reference model and the external command satisfy the condition*

$$(\|K\| + \lambda_g\|K_0\|)\,\|\boldsymbol{x}_m(t)\| + \|K_0\|\|\boldsymbol{g}(x_m(t))\| + \frac{\|\boldsymbol{r}(t)\|}{\lambda^*} \leq \rho_1$$

and the initial tracking error lies in the ball of a radius ρ_2/γ_A, where

$$\rho_2 \left(\|K\| + \lambda_g \|K_0\|\right) \leq d^* + \rho_1,$$

then the system (2) will track the reference model (1) with a bounded error satisfying (29), and the adaptive control (26) will satisfy the input constraint $\|\boldsymbol{v}(t)\| \leq v^*$.

VI. Drone's Dynamic Model

A. Equations of Motion

The dynamics of the multi-rotor vehicle's center of mass in the East-North-Up Earth (inertial) frame (F_E) are given by

$$\begin{aligned} \dot{\boldsymbol{r}}(t) &= \boldsymbol{v}(t) \\ m\dot{\boldsymbol{v}}(t) &= R_{B/E}(t)\boldsymbol{e}_3^B T(t) + \boldsymbol{f}_D(t) + m\boldsymbol{g}\,, \end{aligned} \tag{32}$$

where $\boldsymbol{r}(t) = [x(t)\ y(t)\ z(t)]^\top$ is the position of the center of mass in F_E, $\boldsymbol{v}(t) = [v_x(t)\ v_y(t)\ v_z(t)]^\top$ is the inertial velocity, m is the mass, $T(t) = \sum_{i=1}^{1=n} f_i(t)$ is the total, where $f_i(t)$ is the thrust generated by the i-th rotor at time t in the positive z-direction in F_B frame ($\boldsymbol{e}_3^B = [0\ 0\ 1]^\top$ is the third unit vector of F_B), $R_{B/E}(t)$ is the rotation matrix from the body frame F_B (Forward-Left-Up) to F_E, $\boldsymbol{f}_D(t)$ is the aerodynamic drag force and $\boldsymbol{g} = [0\ 0\ -g]^\top$ is the gravity acceleration.

The vehicle's rotational dynamics about the center of mass are given in the frame F_B as

$$\begin{aligned} \dot{R}_{B/E}(t) &= R_{B/E}(t)\boldsymbol{\omega}^\times(t) \\ J\dot{\boldsymbol{\omega}}(t) &= -\boldsymbol{\omega}(t) \times J\boldsymbol{\omega}(t) + J_m\omega_m(t)\bar{\boldsymbol{\omega}}(t) + \boldsymbol{\tau}(t) + \boldsymbol{\tau}_D(t)\,, \end{aligned} \tag{33}$$

where $\boldsymbol{\omega}(t) = [p(t)\ q(t)\ r(t)]^\top$ is the angular rate of F_B with respect to the inertial frame F_E expressed in F_B, $J = diag(J_1,\ J_2,\ J_3)$ is the vehicle's inertia matrix (the body frame is aligned with the principal axes of inertia), J_m is the rotor inertia about the axis of rotation (assuming identical for all of them), $\bar{\boldsymbol{\omega}}(t) = [-q(t)\ p(t)\ 0]^\top$, $\omega_m(t) = \sum_{i=1}^{n}(-1)^i\Omega_i(t)$, $\Omega_i(t)$ is the i-th rotor angular rate about its axis of rotation, $\boldsymbol{\tau}(t)$ is the torque generated by the rotors, $\boldsymbol{\tau}_D(t)$ is the aerodynamic rotational drag torque.

B. Atmospheric Effects

The aerodynamic drag force is modeled in the body frame as $\boldsymbol{f}_D^B = [-c_{D_x} v_{a_x}^B |v_{a_x}^B| \quad - c_{D_y} v_{a_y}^B |v_{a_y}^B| \quad - c_{D_z} v_{a_z}^B |v_{a_z}^B|]^\top$, where the drag coefficients c_{D_i} are constant for each axis $i = x, y, z$, $\boldsymbol{v}_a^B(t) = \boldsymbol{v}^B(t) - \boldsymbol{w}^B(t)$ is the vehicle's relative to the air velocity expressed in the body frame, and $\boldsymbol{w}^B(t)$ is the wind inertial velocity expressed in the body frame, and is translated to the inertial frame as $\boldsymbol{f}_D = R_{B/E} \boldsymbol{f}_D^B$. The rotational drag torque is modeled in the body frame as $\boldsymbol{\tau}_D^B = [-c_{\tau_x} \omega_{a_x}^B |\omega_{a_x}^B| \quad - c_{\tau_y} \omega_{a_y}^B |\omega_{a_y}^B| \quad - c_{\tau_z} \omega_{a_z}^B |\omega_{a_z}^B|]^\top$, where coefficients c_{D_i} are constant for each axis $i = x, y, z$, and $\boldsymbol{\omega}_a^B(t) = \boldsymbol{\omega}(t) - \boldsymbol{w}_\omega^B(t)$ is the vehicle's relative to air angular rate expressed in the body frame, which includes the air mass circulation rate (or vorticity) $\boldsymbol{w}_\omega^B(t)$ expressed in the body frame. We refer interested reader to [18] for details.

VII. Multi-rotor Air Vehicle's Control

The objective of the multi-rotor air vehicle control is to design total thrust $T(t)$ and control torque $\boldsymbol{\tau}(t)$ such that the vehicle's position and the yaw angle track the given trajectory $\boldsymbol{r}_c(t)$ and $\psi_c(t)$ in the presence of vehicle's mass and inertia parametric uncertainties and atmospheric disturbances.

First we design a position control algorithm assuming that the trajectory command is filtered through decoupled second order reference model in each direction

$$\ddot{\boldsymbol{r}}_m(t) \;=\; -2 f_m \zeta_m \dot{\boldsymbol{r}}_m(t) - f_m^2 [\boldsymbol{r}_m(t) - \boldsymbol{r}_c(t)] \,, \tag{34}$$

where f_m and ζ_m are the frequency and damping ration of the reference model. For this design, we assume vehicle's mass and the atmospheric drag force, which also includes the wind linear velocities, are unknown and that the control signals are the total thrust, roll and pitch angles, which are constraint as $0 < T_{\min} \leq T \leq T_{\max}$ and $-\varphi^* \leq \phi,\ \theta \leq \varphi^*$, where $T_{\min}$, $T_{\max}$ and φ^* are given limits. We use only velocity dynamics for estimation purposes, which are written as

$$\dot{\boldsymbol{v}}(t) = \frac{1}{m} \boldsymbol{T}(t) + \boldsymbol{s}_v(t) + \boldsymbol{g} \,, \tag{35}$$

where $\boldsymbol{T} = [T_x \; T_y \; T_z]^\top = R_{B/E}(t) \boldsymbol{e}_3^B T(t)$. The prediction model for velocity dynamics, which is

used to estimate mass and the drag force, take the form

$$\dot{\hat{\boldsymbol{v}}}(t) = -2f_m\zeta_m\boldsymbol{v}(t) - f_m^2[\boldsymbol{r}(t) - \boldsymbol{r}_c(t)] + \lambda[\boldsymbol{v}(t) - \hat{\boldsymbol{v}}(t)] \tag{36}$$

with the design of thrust vector as

$$\boldsymbol{T}(t) = \hat{m}(t)\left[-2f_m\zeta_m\boldsymbol{v}(t) - f_m^2[\boldsymbol{r}(t) - \boldsymbol{r}_c(t)] - \hat{\boldsymbol{s}}_v(t)\right] \triangleq \hat{m}(t)\boldsymbol{f}_c(t)\,, \tag{37}$$

where the parameter estimates are updated on-line according to adaptive laws

$$\begin{aligned} \dot{\hat{\boldsymbol{s}}}_v(t) &= \gamma\,\mathrm{Pr}\left(\hat{\boldsymbol{s}}_v(t),\ \tilde{\boldsymbol{v}}(t)\right) \\ \dot{\hat{m}}(t) &= \gamma\,\mathrm{Pr}\left(\hat{m}(t),\ -\tilde{\boldsymbol{v}}^\top(t)\boldsymbol{f}_c(t)\right)\,. \end{aligned} \tag{38}$$

The required total trust and Euler angle commands are obtained from (37) as

$$\begin{aligned} T(t) &= \sqrt{T_x^2(t) + T_y^2(t) + T_z^2(t)} \\ \phi_c(t) &= \arctan_2\left(T_x(t)\cos(\psi(t)) + T_y(t)\sin(\psi(t)), T_z(t)\right) \\ \theta_c(t) &= \arctan_2\left(T_x(t)\sin(\psi(t)) - T_y(t)\cos(\psi(t)), T_z(t)/\cos(\phi_c(t))\right)\,, \end{aligned} \tag{39}$$

Now, we derive the control torque for the rotational dynamics (33) such that the Euler angles $\phi(t),\ \theta(t),\ \psi(t)$ track the reference signals $\phi_c(t),\ \theta_c(t),\ \psi_c(t)$. Here we use time scale separation based backstepping approach for kinematics and define angular rates commands as

$$\begin{aligned} p_c(t) &= c_\phi\left[\phi_c(t) - \phi(t)\right] - c_\psi\left[\psi_c(t) - \psi(t)\right]\sin(\theta(t)) \\ q_c(t) &= c_\theta\left[\theta_c(t) - \theta(t)\right]\cos(\phi(t)) + c_\psi\left[\psi_c(t) - \psi(t)\right]\sin(\phi(t))\cos(\theta(t)) \\ r_c(t) &= -c_\theta\left[\theta_c(t) - \theta(t)\right]\sin(\phi(t)) + c_\psi\left[\psi_c(t) - \psi(t)\right]\cos(\phi(t))\cos(\theta(t))\,, \end{aligned} \tag{40}$$

where $c_\phi > 0,\ c_\theta > 0,\ c_\psi > 0$ are design constants. The adaptive control torques required to track the angular rate commands are defined using the prediction model

$$\dot{\hat{\boldsymbol{\omega}}}(t) = c_{\boldsymbol{\omega}}\left[\boldsymbol{\omega}_c(t) - \boldsymbol{\omega}(t)\right] + \lambda\left[\boldsymbol{\omega}(t) - \hat{\boldsymbol{\omega}}(t)\right] \tag{41}$$

for the angular rate dynamics, which are written as

$$\dot{\boldsymbol{\omega}}(t) = -J^{-1}\boldsymbol{\omega}(t) \times J\boldsymbol{\omega}(t) + J_m\omega_m(t)J^{-1}\bar{\boldsymbol{\omega}}(t) + J^{-1}\boldsymbol{\tau}(t) + \boldsymbol{s}_\omega(t)\,, \tag{42}$$

or component-wise

$$
\begin{aligned}
\dot{p}(t) &= c_{p1}q(t)r(t) + c_{p2}q(t) * \omega_m(t) + s_p(t) + \frac{1}{J_1}\tau_1(t) \\
\dot{q}(t) &= c_{q1}q(t)r(t) + c_{q2}p(t) * \omega_m(t) + s_q(t) + \frac{1}{J_2}\tau_2(t) \\
\dot{r}(t) &= c_{r1}q(t)r(t) + s_r(t) + \frac{1}{J_3}\tau_3(t)\,.
\end{aligned} \tag{43}
$$

The resulting control torques are defined as

$$
\begin{aligned}
\tau_1(t) &= \hat{J}_1(t)\left[c_p\left[p_c(t) - p(t)\right] - \hat{c}_{p1}(t)q(t)r(t) - \hat{c}_{p2}(t)q(t) * \omega_m(t) - \hat{s}_p(t)\right] \triangleq \hat{J}_1(t)f_{pc}(t) \\
\tau_2(t) &= \hat{J}_2(t)\left[c_q\left[q_c(t) - q(t)\right] - \hat{c}_{q1}(t)q(t)r(t) - \hat{c}_{q2}(t)p(t) * \omega_m(t) - s_q(t)\right] \triangleq \hat{J}_2(t)f_{qc}(t) \\
\tau_3(t) &= \hat{J}_3(t)\left[c_q\left[r_c(t) - r(t)\right] - \hat{c}_{r1}(t)q(t)r(t) - \hat{s}_r(t)\right] \triangleq \hat{J}_3(t)f_{rc}(t)\,,
\end{aligned} \tag{44}
$$

where the estimates of corresponding unknown quantities satisfy the adaptive laws

$$
\begin{aligned}
\dot{\hat{\boldsymbol{s}}}_\omega(t) &= \gamma\,\mathrm{Pr}\left(\hat{\boldsymbol{s}}_\omega(t),\ \tilde{\boldsymbol{\omega}}(t)\right) \\
\dot{\hat{J}}(t) &= \gamma\,\mathrm{Pr}\Big(\hat{J}(t),\ \ -diag\left[f_{pc}(t),\ f_{qc}(t),\ f_{rc}(t)\right]\tilde{\boldsymbol{\omega}}(t)\Big) \\
\dot{\hat{c}}_{p1}(t) &= \gamma\,\mathrm{Pr}\left(\hat{c}_{p1}(t),\ q(t)r(t)\tilde{p}(t)\right) \\
\dot{\hat{c}}_{p2}(t) &= \gamma\,\mathrm{Pr}\left(\hat{c}_{p2}(t),\ q(t)\omega_m(t)\tilde{p}(t)\right) \\
\dot{\hat{c}}_{q1}(t) &= \gamma\,\mathrm{Pr}\left(\hat{c}_{q1}(t),\ p(t)r(t)\tilde{q}(t)\right) \\
\dot{\hat{c}}_{q2}(t) &= \gamma\,\mathrm{Pr}\left(\hat{c}_{q2}(t),\ p(t)\omega_m(t)\tilde{q}(t)\right) \\
\dot{\hat{c}}_{r1}(t) &= \gamma\,\mathrm{Pr}\left(\hat{c}_{q1}(t),\ p(t)q(t)\tilde{r}(t)\right)\,.
\end{aligned} \tag{45}
$$

VIII. Simulation Results

Using the dynamic model of DJI S1000 octocopter, we conducted MatLab simulations to demonstrate the performance of M-MRAC in the presence of input constraints, unknown mass and inertia parameters, and atmospheric wind. The simulation setup follows design steps of section VII with constant position $\boldsymbol{r}_c$ and sinusoidal yaw angle commands. For this simulations we use the following parameters: $m = 8\ kg$, $J = diag(0.3245,\ 0.3245,\ 0.4616)\ kg.m^2$, $T_{\min} = 5\ N$, $T_{\max} = 200\ N$, $\varphi^* = 45$ degrees. The wind components are set to $w_x(t) = 7.2\sin(1.5t)$, $w_y(t) = 7.2\sin(1.6t)$, $w_z(t) = 5.7\sin(1.7t)$, $w_p(t) = 0.7\sin(2.5t)$, $w_q(t) = 0.6\sin(2.4t)$, $w_r(t) = 0.5\sin(2.3t)$.

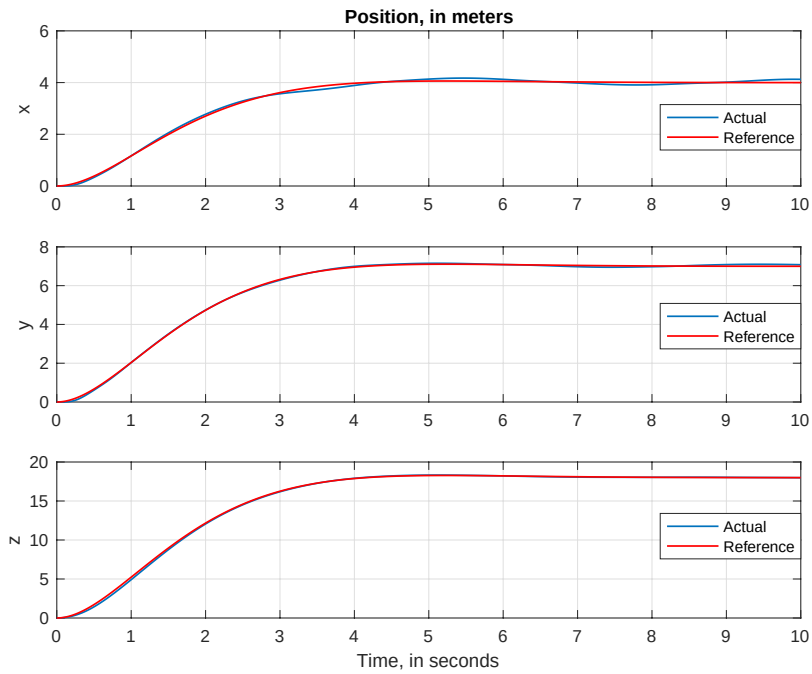

Fig. 1 Reference trajectory tracking time history.

For the first simulation we choose reference model parameters as $f_m = 1$, $\zeta_m = 0.8$, gains for the rate commands are set to 10, and for control torques to 20. The adaptive rate is set to $\gamma = 1000$ and estimation feedback gain to $k = \sqrt{\gamma}$. The reference models and the prediction models are initialized at the system's initial conditions, the adaptive estimates are initialized at zero except for $\hat{m}(0)$, which is set to 5. For the chosen parameters, the set point command $\boldsymbol{r}_c = [4 \;\; 7 \;\; 18]^\top$ satisfies the sufficient condition (31).

Fig. 1 displays the reference trajectory tracking performance of the presented M-MRAC design. A very good tracking can be observed despite the severe disturbance. It can be also observed from Figs. 2 and 3 that the total thrust, roll and pitch angle commands do not exceed the set bounds.

Fig. 4 displays the velocity prediction and reference command tracking performance. It can be observed that very close prediction is generated by the presented adaptive algorithm. Although it is not a primary objective here, but a good reference velocity tracking can be observed as well.

The vehicle's orientation control performance is displayed in Figs. 3 and 5. Here, a very good tracking can be observed as well. Fig. 5 also displays the a very close angular rate prediction by

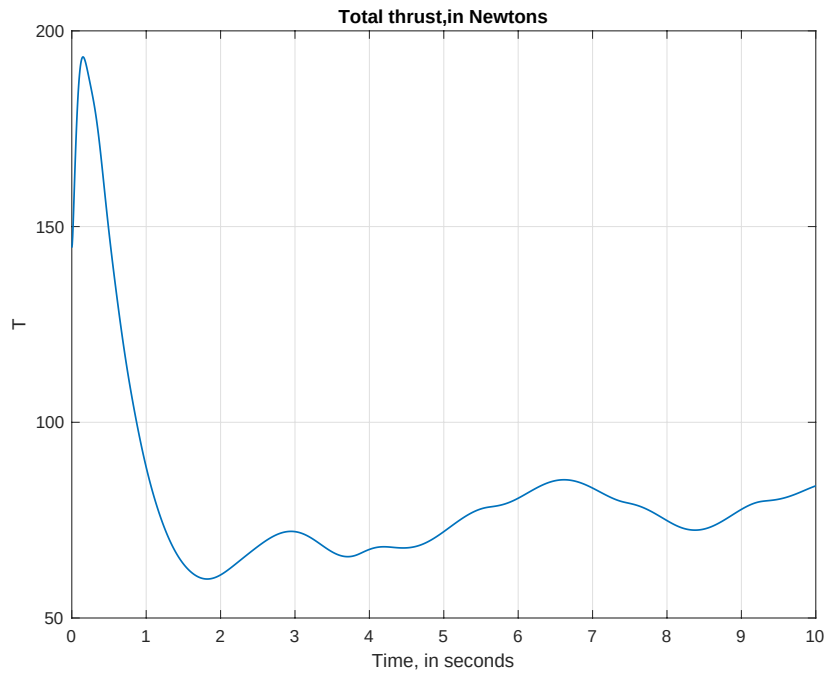

Fig. 2 Total thrust time history.

the presented adaptive algorithm.

In the next simulation, we set the initial condition for the reference model as $\boldsymbol{r}_m(0) = \boldsymbol{r}(0) - [5 \;\; 5 \;\; 5]^\top$, and the initial condition for the prediction model model as $\hat{\boldsymbol{v}}(0) = \boldsymbol{v}(0) - [1.5 \;\; 1.5 \;\; 1.5]^\top$, which still satisfy the sufficient condition (31). It can be observed from Figs. 6, 7 and 8 that the initialization error has little effect on the performance.

In the final set of simulations we speedup the reference model by setting its natural frequency to $f_m = 1.4$, which causes the reference state to violate the sufficient condition (31). It can be seen from Figs. 9 and 10 that the control signals $T(t)$, $\phi_c(t)$ and $\theta_c(t)$ hit the saturation bounds, which results in instability displayed in Fig. 11

IX. Conclusion

We have presented modified model reference adaptive control (M-MRAC) performance for input constraint multi-input multi-output nonlinear dynamical systems with parametric uncertainties and bounded external disturbances. A sufficient condition has been derived, which specificities the region of attraction in the space of initialization errors, design parameters and external commends.

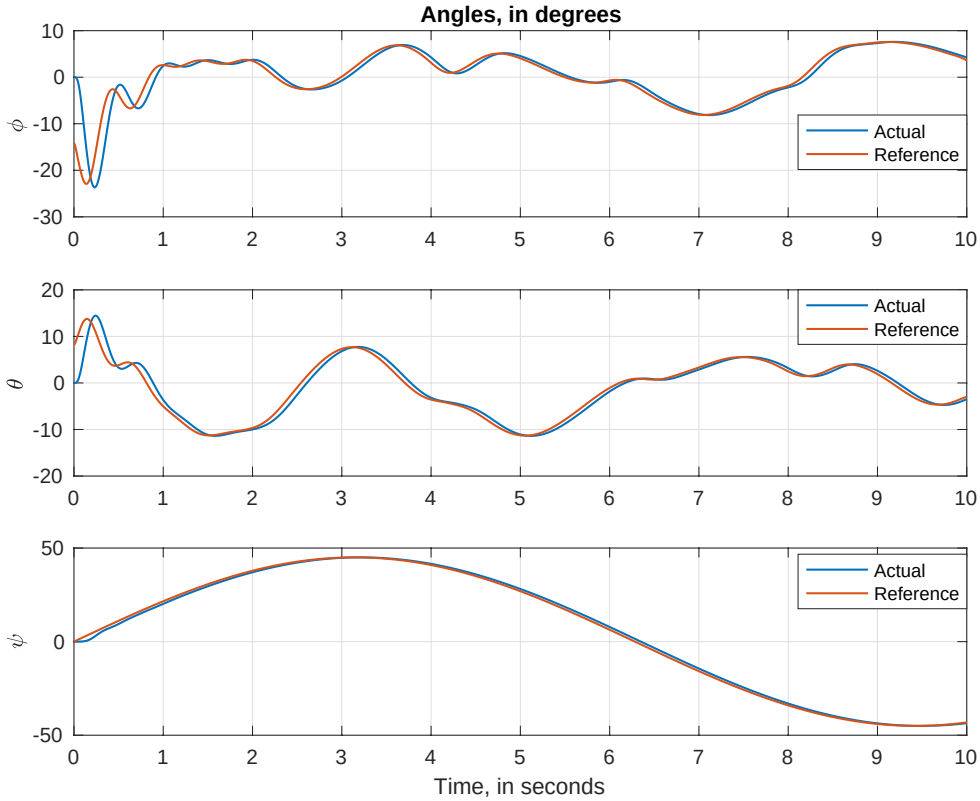

Fig. 3 Euler angles reference command tracking time history.

The approach has been applied to thrust controlled multi-rotor air vehicles operating in the urban environment. It is shown that the designed controller can provide a good tracking of a given trajectory in the unknown urban wind field, assuming that the maximum thrust generated by rotors is known. The algorithms have been verified using simulations.

Acknowledgment

This work was supported by the NASA Ames UAS Traffic Management (UTM) Sub-project, under the NASA's Safe Autonomous Systems Operations (SASO) Project. The authors gratefully acknowledge all members of the SAFE50 team for engaging in many hours of discussions on various topics discussed in this paper.

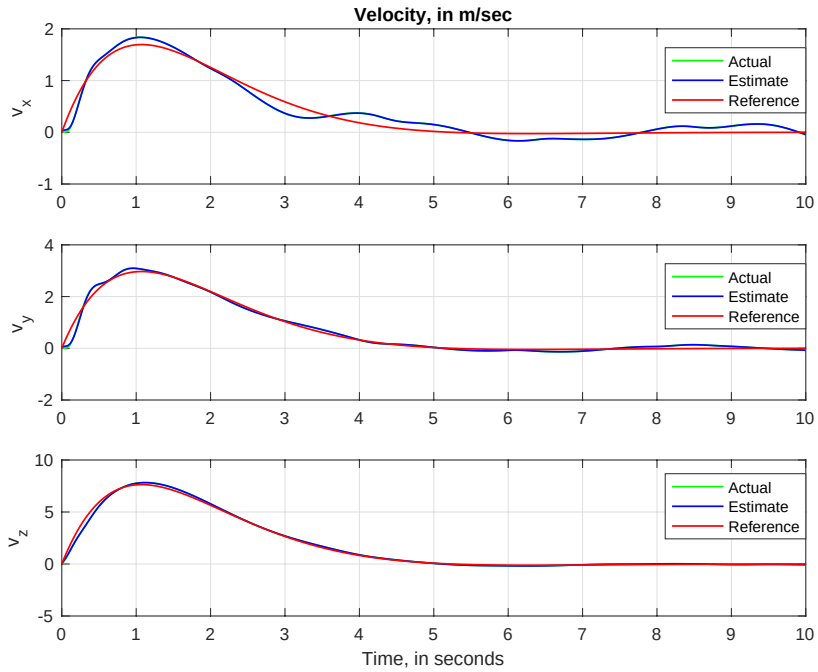

Fig. 4 Velocity estimation and reference command tracking time history.

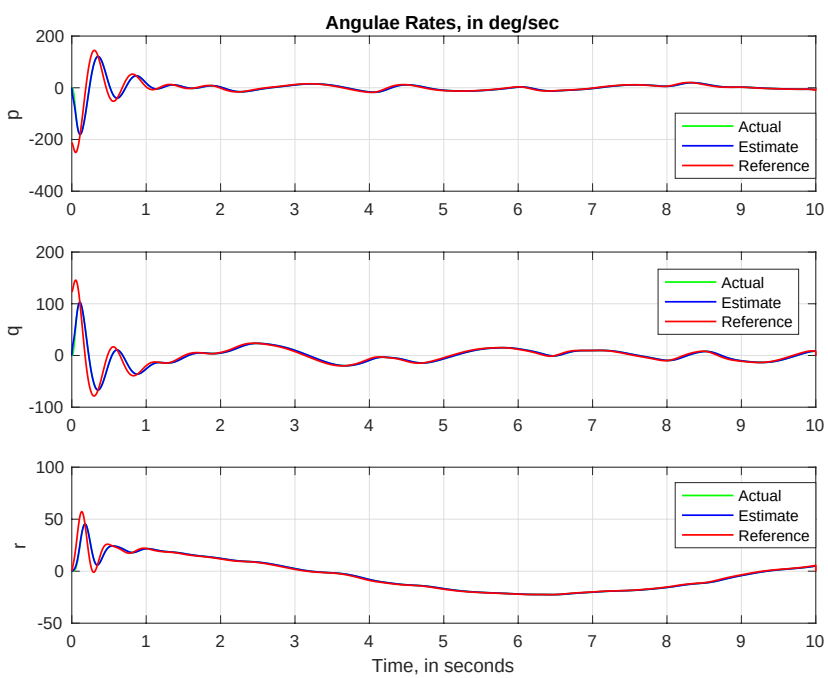

Fig. 5 Angular rate estimation and reference command tracking time history.

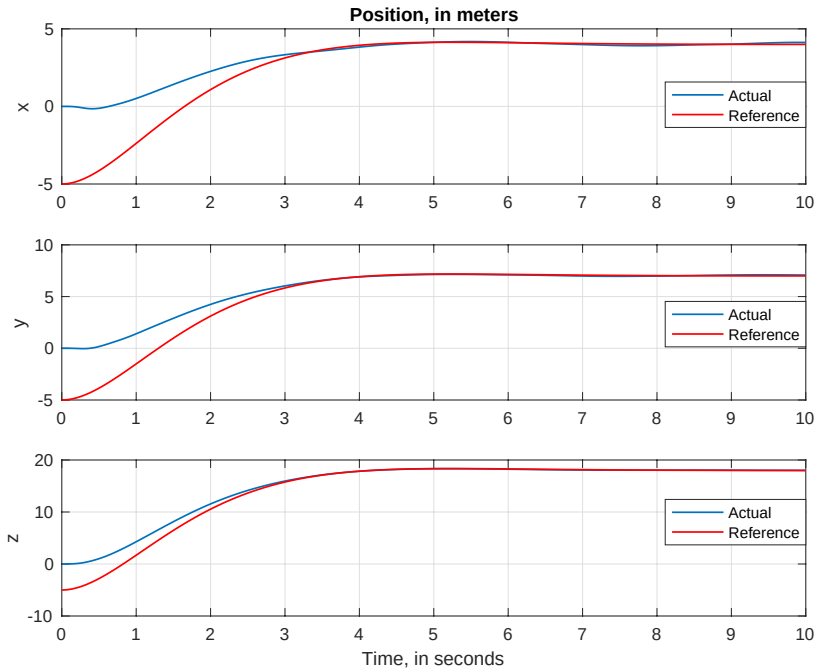

Fig. 6 Reference trajectory tracking time history.

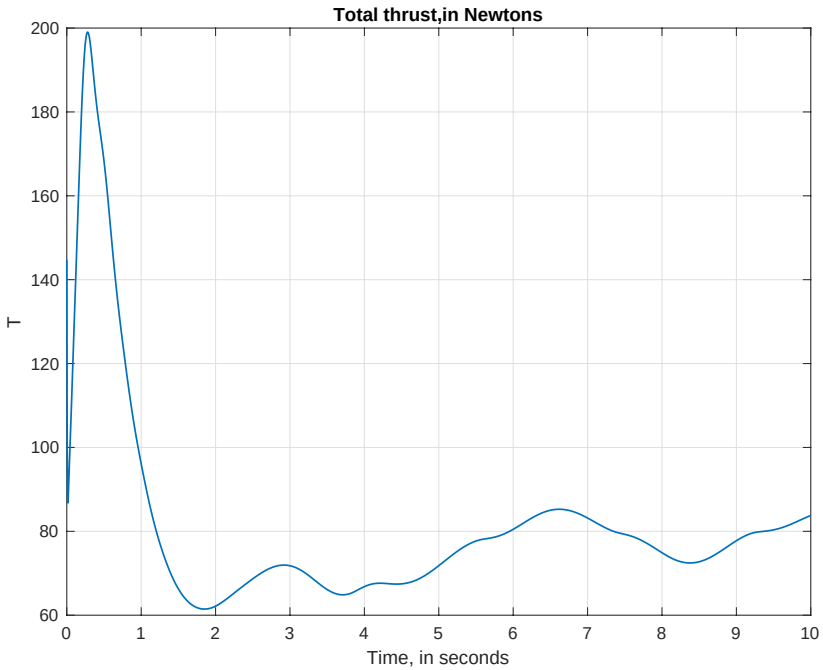

Fig. 7 Total thrust time history.

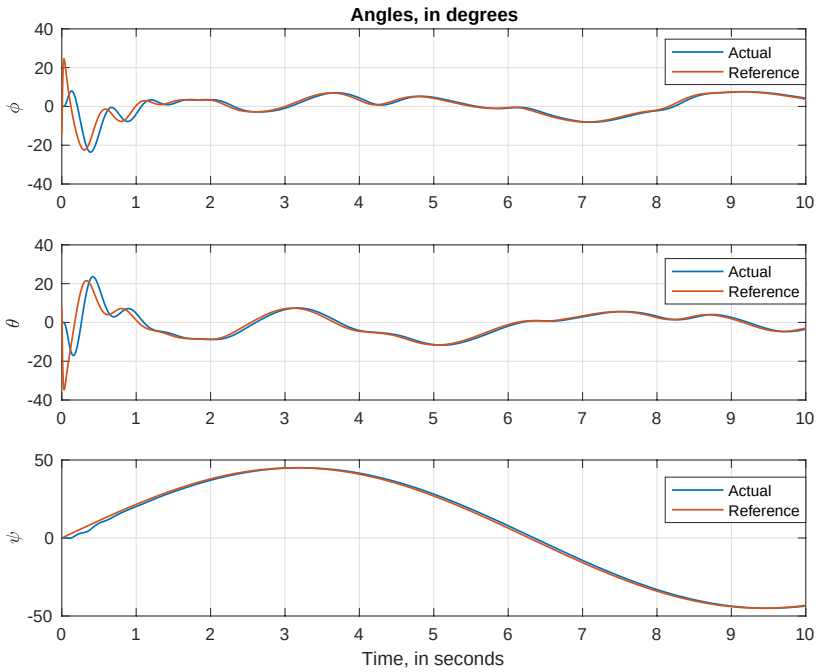

Fig. 8 Euler angles reference command tracking time history.

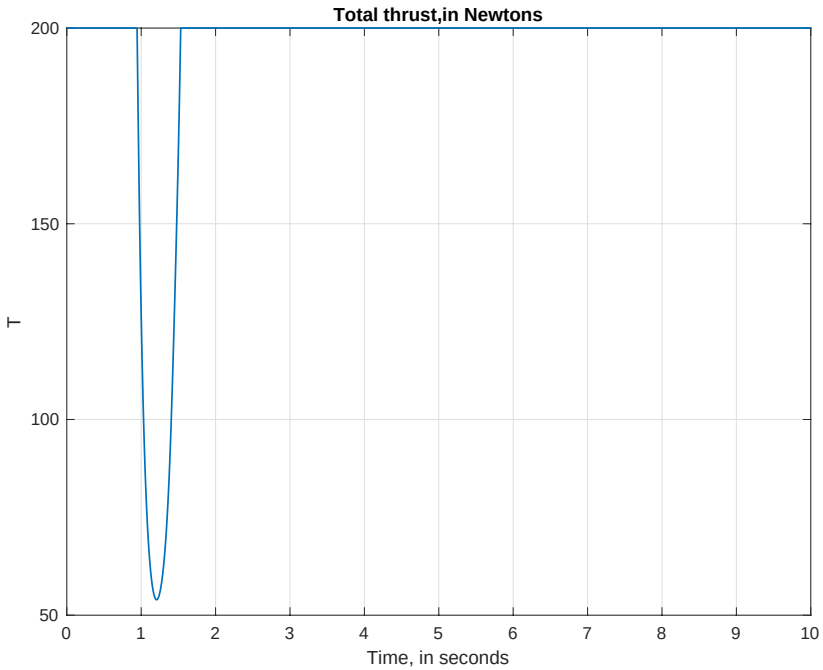

Fig. 9 Total thrust saturation caused by the fast reference model.

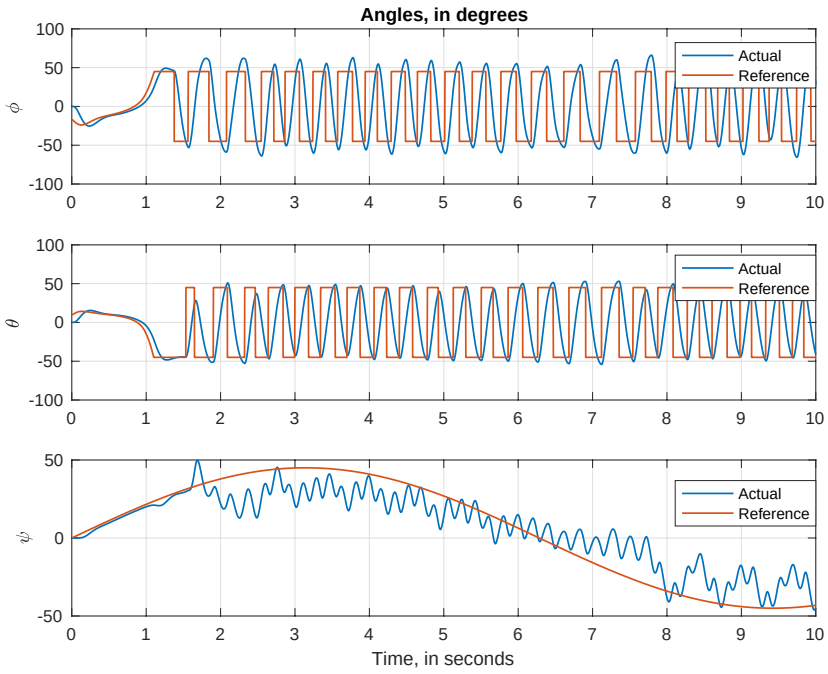

Fig. 10 Euler angle commands saturation caused by the fast reference model.

References

[1] S. M. Adams and C. J. Friedland. A Survey of Unmanned Aerial Vehicle (UAV) Usage for Imagery Collection in Disaster Research and Management. *In Proc. of the 9th International Workshop on Remote Sensing for Disaster Response*, 2011.

[2] V. Adetola, D. D. Adn, and M. Guay. Adaptive model predictive control for constrained nonlinear systems. *Systems and Control Letters*, 58:320–326, 2009.

[3] D. Bernstein and A.A. Michel. Chronological Bibliography on Saturating Actuators. *International Journal of Robust and Nonlinear Control*, (5):375–380, 1995.

[4] M. Chen, G. Tao, and B. Jiang. Adaptive NN Control of a Class of Nonlinear Systems With Asymmetric Saturation Actuators. *IEEE Transactions on Neural Networks and Learning Systems*, 26(9):2086–2097, September 2015.

[5] H. M. Do, T. Bassar, and J. Y. Choi. An Anti-windup Design for Single Input Adaptive Control Systems in Strict Feedback Form. *In Proc. of the American Control Conference, Boston, MA*, pages 2551–2556, 2004.

[6] E.N.Johnson and A.J.Calise. Limited Authority Adaptive Flight Control for Reusible Launch Vehicles. *AIAA Journal of Guidance, Control, and Dynamics*, 26(6):906–913, 2003.

[7] G. Hoareau, J. J. Liebenberg, J. G. Musial, and T. R. Whitman. Package Transport by Unmanned

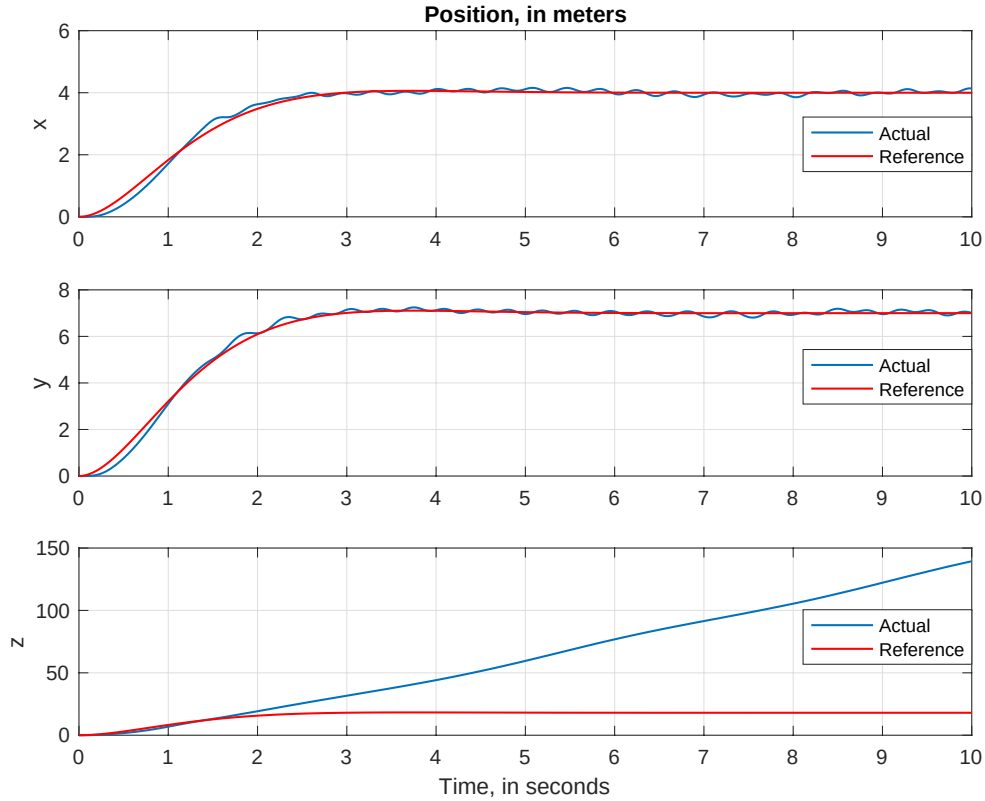

Fig. 11 Instability of the system caused by the fast reference model.

Aerial Vehicles. *US Patent 9731821*, August 15, 2017.

[8] E. N. Johnson and A. J. Calise. Neural Network Adaptive Control of Systems with Input Saturation. *American Control Conference*, 2001.

[9] J. Katrasnik, F. Pernus, and B. Likar. A Survey of Mobile Robots for Distribution Power Line Inspection. *IEEE Transactions on Power Delivery*, 25(1):485–493, 2010.

[10] Y. H. Kim and F. L. Lewis. Reinforcement adaptive control of a class of neural-net-based friction compensation control for high speed and precision. *IEEE Transactions on Control Systems Technology*, 8(1):118–126, January 2000.

[11] E. Lavretsky and N. Hovakimyan. Stable Adaptation in the Presence of Actuator Constraints with Flight Control Applications. *AIAA Journal of Guidance, Control, and Dynamics*, 30(2):337–345, 2007.

[12] A. Leonessa, W. M. Haddad, T. Hayakawa, and Y. Morel. Adaptive control for nonlinear uncertain systems with actuator amplitude and rate saturation constraints. *International Journal of Adaptive Control Signal Processing*, 23(1):73–96, 2009.

[13] J Ma, S. S. Ge, Z. Zheng, and D. Hu. Adaptive NN Control of a Class of Nonlinear Systems With

Asymmetric Saturation Actuators. *IEEE Transactions on Neural Networks and Learning Systems*, 26(7):1532–1538, July 2015.

[14] N. Nigam, S. Bieniawski, I. Kroo, and J. Vian. Control of Multiple UAVs for Persistent Surveillance: Algorithm and Flight Test Results. *IEEE Transactions on Control Systems Technology*, 20(5):1236–1251, 2012.

[15] M. Polycarpou, J. Farrell, and M. Sharma. On-line approximation control of uncertain nonliner systems: Issues with control input saturation. *In Proc. of American Control Conference, Denver, CO*, pages 543–548, 2003.

[16] J. B. Pomet and L. Praly. Adaptive Nonlinear Regulation: Estimation from the Lyapunov Equation. *IEEE Trans. Autom. Contr.*, 37(6):729–740, 1992.

[17] V. Stepanyan and K. Krishnakumar. Indirect M-MRAC for Systems with Time Varying Parameters and Bounded Disturbances. *In Proc. of the IEEE Multi-Conference on Systems and Control, Dubrovnik, Croatia*, 2012.

[18] Vahram Stepanyan and Kalmanje Krishnakumar. Estimation, Navigation and Control of Multi-Rotor Drones in an Urban Wind Field. *In Proc. of the AIAA Information Systems-AIAA Infotech @ Aerospace, Grapevine, TX*, 2017.

[19] C. Wen, J. Zhou, Z. Liu, and H. Su. Robust Adaptive Control of Uncertain Nonlinear Systems in the Presence of Input Saturation and External Disturbance. *IEEE Transactions on Automatic Control*, 56(7):1672–1678, 2011.

[20] J. Yan, D. Antônio dos Santos, and D. S. Bernstein. Adaptive control with convex saturation constraints. *IET Control Theory and Applications*, 8(12):1096–1104, August 2014.

[21] Z. Zhao, Z. Zheng, M. Zhu, and Z. Wu. Adaptive fault tolerant attitude tracking control for a quadrotor with input saturation and full-state constraints. *In Proc. of 13th IEEE International Conference on Control and Automation (ICCA), Ohrid, Macedonia*, 13(2):868–875, July 3-6 2017.

[22] Y. Zhou, M. Chen, and C. Jiang. Robust Tracking Control of Uncertain MIMO Nonlinear Systems with Application to UAVs. *IEEE/CAA Journal of Automatica Sinica*, 2(1):25–32, January 2015.